Accepted Manuscript

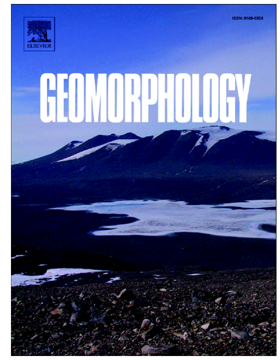

GIS-based evaluation of diagnostic areas in landslide susceptibility analysis of Bahluieț River Basin (Moldavian Plateau, NE Romania). Are Neolithic sites in danger?

Ionut Cristi Nicu, Andrei Asăndulesei

PII: S0169-555X(18)30171-5
DOI: doi:10.1016/j.geomorph.2018.04.010
Reference: GEOMOR 6381

To appear in: *Geomorphology*

Received date: 25 January 2018
Revised date: 13 April 2018
Accepted date: 23 April 2018

Please cite this article as: Ionut Cristi Nicu, Andrei Asăndulesei , GIS-based evaluation of diagnostic areas in landslide susceptibility analysis of Bahluieț River Basin (Moldavian Plateau, NE Romania). Are Neolithic sites in danger?. The address for the corresponding author was captured as affiliation for all authors. Please check if appropriate. Geomor(2017), doi:10.1016/j.geomorph.2018.04.010

GIS-based evaluation of diagnostic areas in landslide susceptibility analysis of Bahluieț River Basin (Moldavian Plateau, NE Romania). Are Neolithic sites in danger?

Ionut Cristi Nicu [1, 2], Andrei Asăndulesei [1]

1. Interdisciplinary Research Department – Field Science, Alexandru Ioan Cuza University of Iasi, St. Lascar Catargi 54, 700107, Iasi, Romania

2. School of Humanities and Creative Arts, Faculty of Education, Humanities and Law, Flinders University, Sturt Road, Bedford Park SA 5042, GPO Box 2100, Adelaide SA, Australia

nicucristi@gmail.com, +40745868154

orcid.org/0000-0001-6451-341x – Ionut Cristi Nicu

orcid.org/0000-0001-8781-0468 – Andrei Asăndulesei

Abstract

The aim of this study is to compare the predictive strenghtness of different diagnostic areas in determining landslide susceptibility using frequency ratio (FR), statistical index (SI), and analytic hierarchy process (AHP) models in a catchment from the northeastern part of Romania. Scarps (point), landslide areas (polygon), and middle of the landslide (point) have been tested and checked in regards to their performance. The three statistical models have been employed to assess the landslide susceptibility using eleven conditioning factors (slope angle, elevation, curvature, lithology, precipitations, land use, topographic wetness index (TWI), landforms, aspect, plan curvature and distance to river). The three models were validated using the receiver operating characteristic (ROC) curves and the seed cell area index (SCAI) methods. The predictive capability of each model was established from the area under the curve (AUC), for FR, SI and AHP; the values are 0.75, 0.81 and 0.78 (using polygon as diagnostic area), respectively. Among the three methods used, SI had a better predictability. When it comes to the predictability values regarding the diagnostic areas, the landslide area (polygon) proves to have the highest values. This results from the entire surface of the landslide being taken into account when validating the data. Approximately 70% of the Neolithic sites are located in areas with high and very high susceptibility to landslides, meaning that they are in danger of being destroyed in the future. The final susceptibility maps are useful in hazard mitigation, risk reduction, a sustainable land use planning, evaluation of cultural heritage integrity, and to highlight the most endangered sites that are likely to be destroyed in the future.

Keywords: frequency ratio, analytic hierarchy process, GIS, Neolithic

1. Introduction

Landslides represent one of the most devastating geomorphological processes when it comes to the natural change and associated material losses. Hilly areas, especially those located at the transition between plain and plateau, represent areas with a high probability of developing slope processes (e.g. landslides) (Guzzetti et al., 2005). To comprehend the spatial pattern behind a landslide, a set of landslide environmental and triggering factors is needed. According to van Westen et al. (2008) spatial data include environmental elements (aspect, slope, curvature), soil characteristics (parent material, soil classes and types), geology (faults, rock type), geomorphology (geomorphological units, terrain mapping units), hydrology (distance to stream), and land-use (pastures, wetlands, orchards, non-productive lands) (Zhang et al., 2016).

Landslide susceptibility represents the likelihood of a landslide occurring in an area, taking into account the local environment and triggering factors (Guzzetti et al., 2005). It estimates "where" a landslide can happen without implying "when". In other words, the estimation of susceptibility is the evaluation of the level of instability in an area without considering the probability of landslide occurrences in absolute and temporal terms (Guzzetti et al., 2016). During the last decade, at an international level, an increasing trend exists in applying statistical modelling in the field of geosciences to a wide range of natural disasters, such as flooding (Cao et al., 2016), rock falls (Shirzadi et al., 2017), fires (Hong et al., 2017), avalanches (Kumar et al., 2016); others are applied for the assessment of human-induced modifications to the landscape (Al-sharif and Pradhan, 2016), cultural heritage (Nicu 2016a), water resources management (Mousavi et al., 2017), waste management (Taboada-Gonzáles et al., 2014), and renewable energy (Ahmad and Tahar, 2014).

This study aims to employ landslide susceptibility in the field of cultural heritage (Neolithic archaeological sites from Bahluet river basin, northeastern Romania). The Bahluieț river basin was chosen because of the high density of Neolithic settlements. A significant number of studies deal with the assessment of landslide susceptibility; to do so, four significant steps have been identified: 1) mapping previous landslides from the study area, 2) mapping certain geological/geomorphological environmental factors that could be directly related with slope failures, 3) assessing the correlation of those factors with landslides, 4) individualise the study area into units with different landslide susceptibility and validation of the landslide susceptibility maps by using receiver operating curves (ROC curves) and seed cell area index (SCAI) (Clerici et al., 2002; Zhang et al., 2016). Another two points could be added towards the approach on cultural heritage: 5) identifying which of the cultural heritage sites are located in areas with high and very high susceptibility to landslides, 6) analysing the most important sites from a geomorphological, geophysical, and archaeological point of view.

Statistical modelling of natural processes became a necessity and a desideratum because more and more studies use statistical modelling to approximate reality and to make predictions from this approximation. Frequency ratio (FR), analytic hierarchy process (AHP), and statistical index (SI) are among the most common methods used to predict landslide susceptibility (Althuwaynee et al., 2014; Nicu, 2018a). The qualitative and quantitative assessment of landslide susceptibility made great progress over the last decade because of an increase in computing capacity and programming (Guzzetti et al., 1999; Chen et al., 2016; Aburas et al., 2017), as well new measurement techniques (Choi et al., 2012; Romanescu et al., 2012).

Qualitative methods, based on the opinion of an individual or a group of experts, are used on landslide inventory and historical materials: experts identify landslides, determine the main conditioning factors, and evaluate sites with similar environmental characteristics. One of the most common qualitative methods is AHP (Saaty, 1977; Myronidiset al., 2016; Wu et al., 2016) and weighted linear combination (WLC) (Akgün et al., 2008). The limitation of this method, however is related to the subjective judgement of the expert(s). To avoid the limitations related to this method in mapping landslide susceptibility, they are used together with one or more quantitative methods (Pourghasemi et al., 2013; Althuwaynee et al., 2014; Shahabi et al., 2014; Chen et al., 2016; Patriche et al., 2016; Zhou et al., 2016; Abedini et al., 2017; Pawluszek and Borkowski, 2017; Nicu, 2018a).

Quantitative methods employ mathematical models to estimate the probability of slope failure in a certain area (Guzzetti et al., 1999). The key to a reliable model is a complete inventory of present landslides, along with the past landslides (Samia et al., 2017). Quantitative methods include logistic regression (LR) (Dailey and Fuhrmann, 2017), binary logistic regression (BLR) and stochastic gradient treeboost (SGT) (Lombardo et al., 2015), frequency ratio (FR), statistical index (SI) and weights of evidence (WOE) (Razavizadeh et al., 2017), WOE, fuzzy logic and FR (Vakhshoori and Zare, 2016), FR and evidential belief function (EBF) (Zhang et al., 2016), FR and index of entropy (IOE) (Youssef et al., 2014), FR, LR and artificial neural networks (ANN) (Pradhan and Lee, 2010), improved self-organizing linear output (SOLO), support vector machine (SVM) and LR (Lin et al., 2017), LR, AHP and combined fuzzy and support vector machine (F-SVM) (Meng et al., 2016), etc.

As described above, multiple studies apply statistical modelling to landslide susceptibility; studies are very limited, however, in applying statistical modelling to assess landslide susceptibility on cultural heritage sites (Klimeš, 2013; Sdao, 2013; Nicu 2017a; Nicu, 2018a, b). Those that exist cover small catchments or punctual case studies. The spread and the high density of cultural heritage sites (as it is in the northeastern part of Romania with Neolithic settlements) requires a regional scale landslide susceptibility study (Nicu 2016b). Cultural heritage around the world is in danger (Nicu 2017b) from natural hazards and anthropic pressure (Nicu 2017c). Sites located in the Moldavian Plateau of northeastern Romania are no exception (Niculiță and Mărgărint, 2017).

Among European states, Romania has one of the highest landslide-prone areas (Bălteanu et al., 2010); the Moldavian Plateau (Fig. 1a) has been recognised as being most susceptible to landslides. Moldavian Plateau, with a total area of 4534.7 km^2, has a density of 1.02 landslides per km^2, (Niculiță et al., 2016). The studies regarding landslide susceptibility in Romania has highlighted a large potential (Mărgărint et al., 2013; Armaș et al., 2014; Mihai et al., 2014; Patriche et al., 2016; Roșca et al., 2016).

This study aims to test and compare the predictive variability of different diagnostic areas (scarps – point, landslide areas – polygon, and middle of landslide – point) in determining landslide susceptibility using FR, SI, and AHP models in a catchment from northeastern part of Romania. The performance of each diagnostic area was tested; the validation results and the predictability strenghtness were analysed and discussed. Previous studies regarding the role of diagnostic areas in the assessment of landslide susceptibility mapping have shown that using landslide scarp offers better results than of using landslide area (Xu et al., 2012; Rotigliano et al., 2011). Both qualitative and quantitative methods will be employed.

The final landslide susceptibility maps will be useful for future cultural heritage preservation and protection, risk reduction, hazard mitigation, and sustainable land development policies at the regional scale. Three important Neolithic sites have been analysed in detail. For two of them, a geophysical survey was employed to determine the precise surface of the settlement (one of them is a newly discovered site). The year 2018 is designated the European Year of Cultural Heritage, therefore, our efforts must be redirected towards the present state and evaluation of cultural heritage, and future preservation towards natural hazards. The study undertaken by Margottini et al., 2015, has shown the importance of modern monitoring techniques in the assessment and proposal of ecosystem-based mitigation measures.

2. Study area

Bahluieț river basin is located in the northeastern part of Romania (Fig. 1b) and has a surface of 550 km^2. Bahluieț River has a length of 50 km, an average slope of 13%, sinuosity coefficient of 1.23, and average catchment altitude of 163 m. (Romanescu and Stoleriu, 2017). Lithologically, the Bessarabian deposits (clay marls with intrusions of sand) of Sarmatian age dominate the basin. The high friability and fine granulation of these deposits have led to the occurrence of geomorphological processes, especially landslides. Quaternary deposits of Pleistocene age are located within the Valea Oii catchment and at the junction of Bahlueț River into Bahlui River; Holocene deposits are located along the Bahlueț River and stretch upstream Goești, Sinești, and Hărpășești river basins (Macarovici and Turculeț, 1956) (Fig. 2a).

The main relief sub-units of Bahlueț basin are highlighted in Fig. 1b. From a climatic point of view, the area belongs to the continental temperate with excessive influences, which is manifested through periods of drought and heavy rainfall. Precipitation ranges between 500 – 700 mm/year, with higher values in the western plateau area and Coasta Iașilor, and lower in the middle part of the basin; the average annual temperature is between 8.3 – 9.6 °C (Minea, 2012). Within the Bahlueț basin, the area occupied by landslides represents 23% of the total surface, being mainly distributed south of Bahlueț River, especially in Dumești Hillocks and Coasta Iașilor. Within the area are two towns (Tîrgu Frumos and Podu Iloaiei) and 52 villages (Fig. 1b).

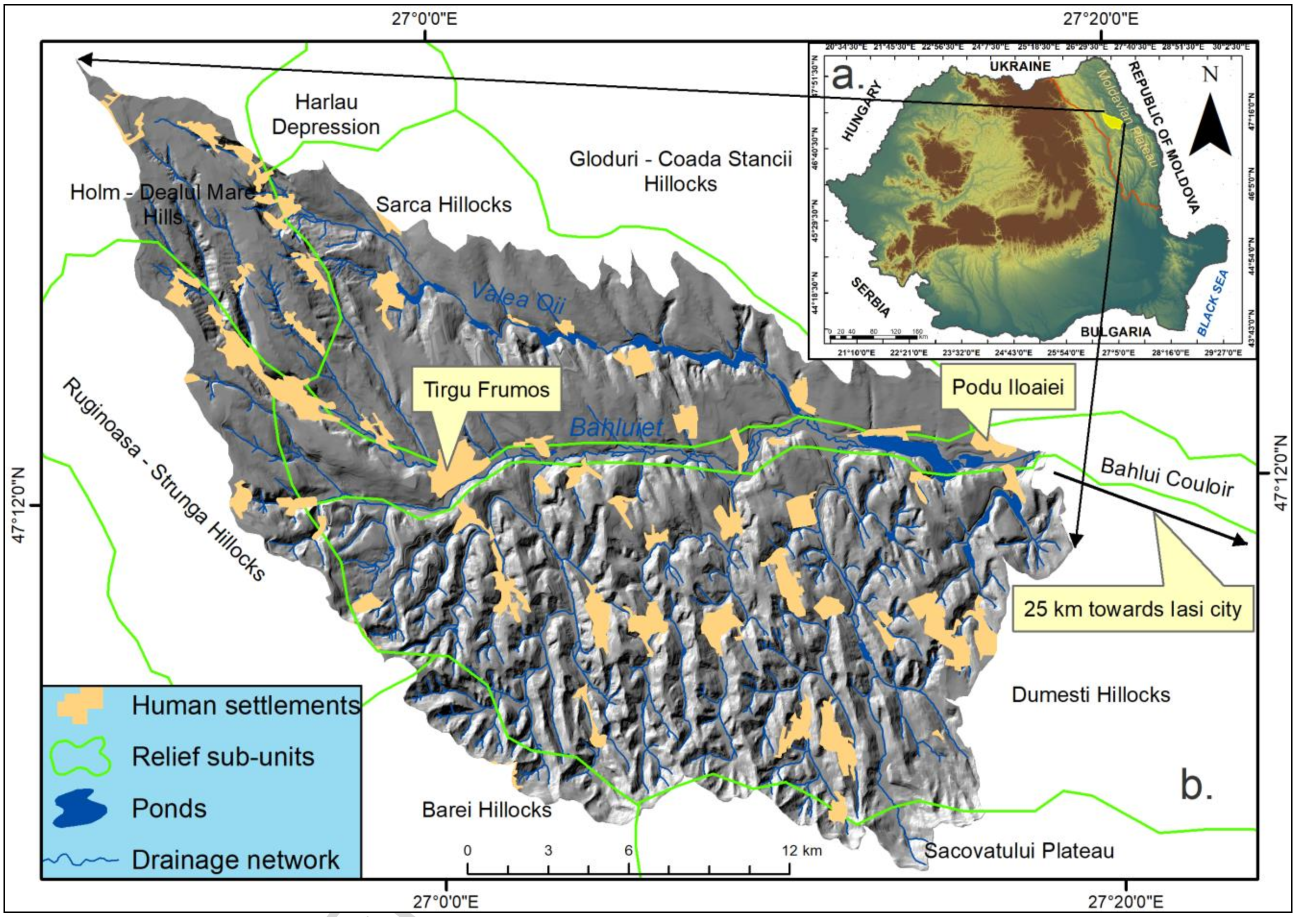

Figure 1. a. Location of Moldavian Plateau, b. Geographic location of the study area in Romania, Iași County context. Highlighted are the main geographical sub-units and cities

3. Archaeological background

Neolithic sites from the northeastern part of the country represent important cultural heritage assets (Monteiro et al., 2015). Bahluieț basin represents the typical landscape in which Neolithic culture could flourish; representative for this part of the country is the Cucuteni culture, one of the most iconic prehistoric cultures of Eastern Europe (Monah, 1985; Lazarovici, 2009). Cucuteni culture is part of the well-known Cucuteni-Ariușd-Trypillia Cultural Complex (covering approximately 350,000 km^2) on the territory of today Romania, Republic of Moldova and Ukraine (Monah, 1985; Lazarovici, 2009; Nicu, 2016b; Asăndulesei, 2017).

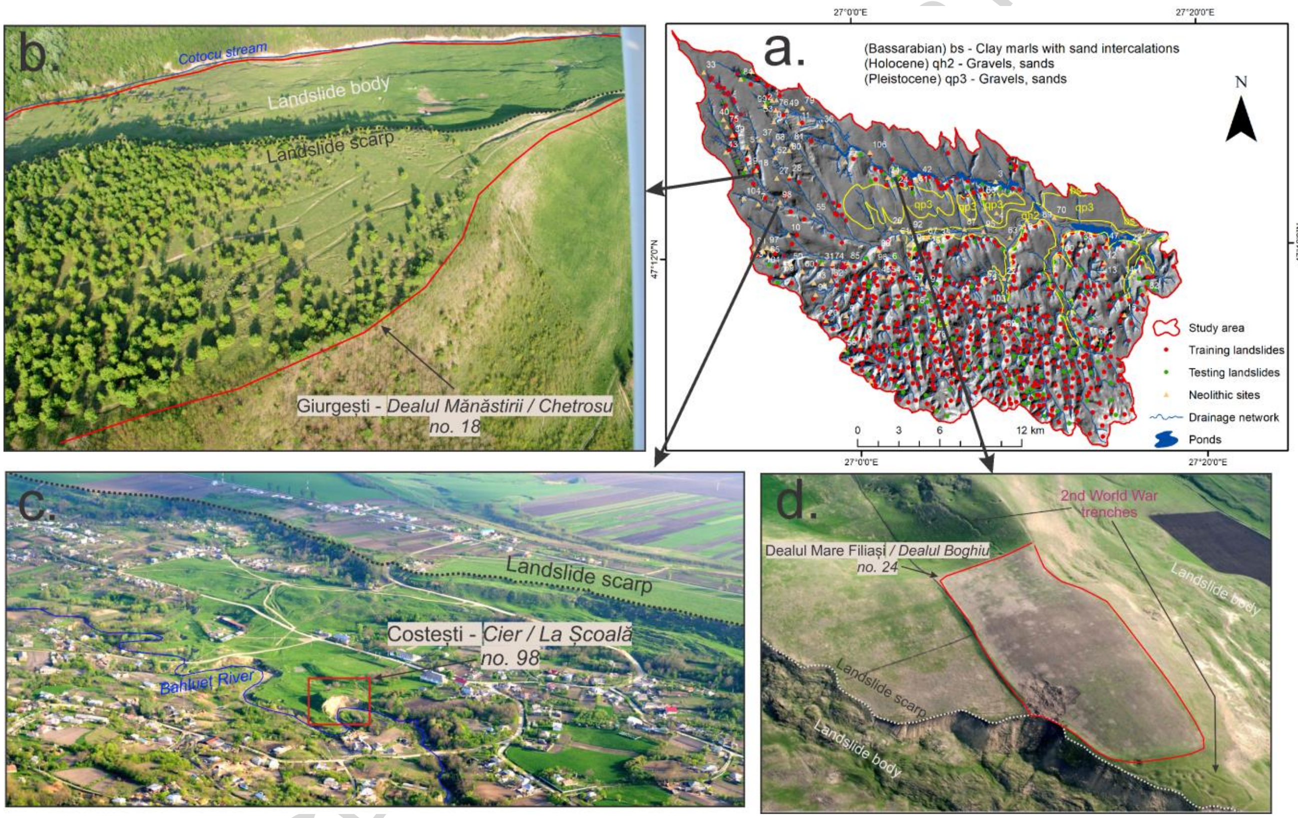

Figure 2. a. The location of testing and training data used for the LSI. Neolithic sites are marked with purple dots. b, c, d. Examples of Neolithic sites affected by landslides: b. The site of Giurgești (*Dealul Mănăstirii / Chetrosu*, no.18), c. The site of Costești (*Cier / La Școală*, no. 98), d. The site of Dealul Mare (*Filiași / Dealul Boghiu*), no. 24

High relief (platforms, hills, terraces) represented the main landform in determining the placement of settlements (Monah, 1985; Nicu, 2016b); also they did settle on rivers terraces, alluvial fans, landslides located in the river proximity on low to medium altitudes and good visibility (Boghian et al. 2016). The total number of Neolithic settlements within Bahlueț river basin is 107 (Fig. 2a). A higher density of settlements occurs in the upper half of the basin. In the lower half of the basin the settlements did not have a good inter-visibility because the territory was highly forested (this means smaller surfaces to be used for agricultural purpose – which was the main occupation of prehistoric people) (Asăndulesei, 2017).

The culture was named after the eponymous settlement from Băiceni village – *Cucuteni Cetățuia* and appeared in western and central Moldavia after the phase III of Precucuteni culture; this site is very important because of its framing as a geoheritage site of the national level (Niculiță and Mărgărint 2017). The discovery of *Cucuteni Cetățuia* settlement in 1884 by the folklorist Th. Burda from Iași marked the beginning of archaeological research in the northeastern part of Romania (Nicu and Romanescu, 2016). As shown in recent studies, the prehistoric people were using the landslide depletion areas as a defensive system (Niculiță et al., 2016), and they might have been aware of the danger that landslides represented for them (Nicu, 2018a).

A few examples of Neolithic sites affected by landslides are given in Fig. 2b, c, d (red lines represent the limit of the settlement). One of the main difficulties is the incompleteness of the archaeological registry; the sites that are registered could be found in the databases of the National Archaeological Registry (RAN), the National Heritage Institute (INP), and the Institute of Cultural Memory (cIMEC).

4. Methods

4.1. FR method – represents a quantitative and recognised method to generate landslide susceptibility maps with a high accuracy (Choi et al., 2012; Shahabi et al., 2014; Vakhshoori and Zare, 2016; Zhang et al., 2016). The method is based on the observed relationship between the distribution of landslides and individual landslide-induced factors. To determine the frequency ratio for each factor class (with the help of Eq. 1), the ratio between landslide occurrence and non-occurrence was calculated (Tab. 1, column 6).

$$FR = (E / F) / (M / L) \qquad \text{(Eq. 1)}$$

Where E is the number of pixels with the landslide for each factor, F is the total number of landslides, M is the number of pixels in the class area, and L is the total number of pixels (Lee and Pradhan, 2007). The weights of each factor were obtained and by summarising the weights the landslide susceptibility index (LSI) was calculated with the following equation (Eq. 2):

$$LSI = \Sigma\, FR_i \qquad \text{(Eq. 2)}$$

Table 1. Frequency ratio and statistical index models for all the conditioning factors

Conditioning factor	Class	No. of pixels in domain	Pixels %	Landslide points	Landslide points %	Frequency Ratio (FR)	Statistical Index (SI)
Altitude (m)	50.2 – 100	3,363,707	15.32	1,175	7.69	0.17	-0.32
	101 – 200	14,319,872	65.21	12,150	79.54	0.41	0.02
	201 – 300	2,775,150	12.64	1,525	9.98	0.27	0.22

	301 – 400	1,412,791	6.43	425	2.78	0.15	-0.62
	> 401	89,623	0.41	0	0	0	-
Slope angle (degrees)	0 – 3	8,873,175	40.40	150	0.98	0	-0.88
	3 – 7	6,894,280	31.39	3,550	23.24	0.15	-0.04
	7 – 14	4,984,204	22.70	9,375	61.37	0.44	0.36
	> 14	1,209,484	5.51	2,200	14.40	0.40	0.41
Curvature	Concave	385,283	1.75	475	3.11	0.39	0.24
	Flat	21,045,116	95.83	14,150	92.64	0.21	-0.01
	Convex	530,744	2.42	650	4.26	0.39	0.23
Lithology	Sandstone	4,484,871	20.42	1,825	11.95	0.17	-0.23
	Limestone	904,658	4.12	125	0.82	0.06	-0.21
	Clay, sand	13,191,520	60.07	9,300	60.88	0.29	0.04
	Clay	3,380,094	15.39	4,025	26.35	0.49	0.07
Precipitations (mm/year)	500 – 550	8,512,022	38.76	6,375	41.73	0.31	-0.10
	550 – 600	8,869,166	40.39	6,700	43.86	0.31	0.02
	600 – 650	2,375,521	10.82	1,500	9.82	0.26	0.29
	650 – 700	2,204,434	10.04	700	4.58	0.31	-0.24
Distance to rivers (m)	< 200	5,691,442	25.92	4,425	28.97	0.21	0.01
	200 – 400	4,960,320	22.59	5,325	34.86	0.29	0.14
	400 – 600	3,950,611	17.99	2,525	16.53	0.17	-0.02
	600 – 800	2,719,905	12.39	1,725	11.29	0.17	-0.06
	800 – 1000	1,838,415	8.37	625	4.09	0.09	-0.15
	> 1000	2,800,450	12.75	650	4.26	0.06	-0.19
Landforms	1	13,718	0.06	0	0	0	0.25
	2	195	0	0	0	0	0.25
	4	281,045	1.28	150	0.98	0.19	0.15
	5	11,409,495	51.95	375	2.45	0.01	-0.75
	6	9,985,547	45.47	14,550	95.25	0.52	0.28

	7	260,802	1.19	200	1.31	0.27	0.19
	9	177	0	0	0	0	0.34
	10	10,164	0.05	0	0	0	0.25
TWI	-7 – -2	568,058	2.59	250	1.64	0.24	0.02
	-1 – -0.1	44,494	0.20	25	0.16	0.31	-0.42
	0 – 30	18,542,604	84.43	14,975	98.04	0.44	0.05
	> 30	2,805,987	12.78	25	0.16	0	-0.86
Aspect	Flat	3,463,117	15.77	875	5.73	0.04	-0.21
	N	3,664,609	16.69	3,100	20.29	0.13	0.18
	NE	3,457,392	15.74	2,500	16.37	0.11	0.04
	E	2,211,100	10.07	850	5.56	0.06	-0.22
	SE	2,237,844	10.19	650	4.26	0.04	-0.42
	S	2,259,101	10.29	1,125	7.36	0.08	-0.26
	SW	2,359,786	10.75	4,175	27.33	0.27	0.20
	W	1,201,188	5.47	1,050	6.87	0.13	0.15
	NW	1,107,006	5.04	950	6.22	0.13	0.13
Plan curvature	< - 0.56	181,186	0.83	150	0.98	0.34	0.23
	- 0.55 – 0.19	20,506,758	93.38	13,900	91	0.27	-0.02
	> 0.20	1,273,199	5.80	1,225	8.02	0.39	0.21
Land use	1	6,327,670	28.81	4,350	28.48	0.19	0.14
	2	1,992,326	9.07	2,575	16.86	0.36	0.22
	3	9,577,405	43.61	2,875	18.82	0.08	-0.51
	4	4,063,742	18.5	5,475	35.84	0.37	0.22

4.2. SI method – is a bivariate statistic approach which was introduced by van Westen (1997) with the purpose of producing landslide susceptibility models (Pourghasemi et al., 2013; Zhang et al., 2016). The method, recognised for its simplicity and robustness, is recommended for large areas and where the spatial data is limited (Poli and Sterlacchini, 2007). The basic principle of this method is the distribution of landslides in each factor class and is calculated with the help of the following equation

$$SI = \ln (F_{ij} / F) = \ln ((L_{ij} / L_{T}) / (P_{ij} / P_{L})) \quad \text{(Eq. 3)}$$

where SI is the weight of a certain class *i* of factor *j*; F_{ij} represents the landslide density within class *i* of the factor *j*. *F* represents the total landslide density in the area of interest; L_{ij} is the number of landslides in a certain class *i* of the factor *j*. L_T represents the total number of landslides; P_{ij} is the number of pixels in a certain class *i* of factor *j*. P_L represents the total number of pixels in the study area.

Each conditioning factor was combined with the landslide map, in this way the weighting value (SI) was obtained for each parameter class (Tab. 1, column 7). Positive values show a high incidence of landslide occurrence, whereas negative values indicate a very low probability of landslide occurrence.

4.3. AHP method, one of the multiple criteria decision making methods, was established by Saaty in the 1970s (Saaty, 1970). AHP, a qualitative method, is widely used in studies dealing with the evaluation of landslide susceptibility (Myronidis et al., 2016; Wu et al. 2016; Pawluszek and Borkowski, 2017), or is used along with other quantitative methods (Pourghasemi et al., 2013; Althuwaynee et al., 2014; Shahabi et al., 2014; Chen et al., 2016; Patriche et al., 2016; Zhang et al., 2016; Abedini et al., 2017). This method is easy to use, provides measures of judgement consistency, and simplifies preference ratings among criteria using pairwise comparisons or the reciprocal of these; the factors are converted into quantitative methods based on expert opinion (Saaty, 2000). The weights of the factors were obtained based on expert analysis, using scoring criteria based on significance. After the normalised weights are calculated for each factor (Table 2), the consistency is checked by calculating the consistency ratio (CR). To calculate CR, the consistency index (CI) has to be determined in advance with the help of Eq. 4.

$$CI = \lambda - n \,/\, n - 1 = 11.79–11/11\text{-}1 = 0.79/10 = 0.079 \qquad \text{(Eq. 4)}$$

Where λ represents the average number of the consistency measure obtained in Tab. 1, column 14, and *n* is the number of criteria used in the study.

Table 2. Derivation of weights for each conditioning factor with the help of AHP

Factor	**Slope**	**Elevation**	**Curvature**	**Lithology**	**Precipitations**	**Land use**	**TWI**	**Landforms**	**Aspect**	**Plan curvature**	**River distance**	**Weights**	**Consistency measure**
Slope	1	3	3	1	2	1	5	2	2	5	3	**18.9**	11.2
Elevation	1/3	1	2	1/3	2	1/5	3	1/2	1/2	1/2	1/2	**6.5**	11
Curvature	1/3	1/2	1	1/2	1	1/3	1	1/3	2	2	1/3	**5.7**	11.5
Lithology	1	3	2	1	2	1	3	1	3	3	2	**13.1**	12.8
Precipitations	1/2	1/2	1	1/2	1	1/2	2	1/3	2	2	1/2	**6.5**	11.7
Land use	1	5	3	1	2	1	3	1/2	3	2	1	**13.5**	12.1
TWI	1/5	1/3	1	1/3	1/2	1/3	1	1/4	1/2	1/2	1/4	**3.3**	11.7
Landforms	1/2	2	3	1	3	2	4	1	2	2	1	**13.5**	11.8
Aspect	1/2	2	1/2	1/3	1/2	1/3	2	1/2	1	1	1/3	**5.5**	11.9
Plan curvature	1/5	2	1/2	1/3	1/2	1/2	2	1/2	1	1	1/2	**5.2**	12.3
River distance	1/3	2	3	1/2	2	1	4	1	3	2	1	**12.1**	11.1
Sum	5.9	21.3	20	6.7	16.5	8.2	30	7.9	20	21	10.4	-	11.79 (average)

Consistency ratio: 0.05231

The CR was obtained by using Eq. 5, namely by dividing CI and RI (random consistency index depending on the order of the matrix is given in Tab. 3)

CR = CI / RI = 0.079 / 1.51 = 0.05 (Eq. 5)

Table 3. Random Consistency Index values (RI)

n	1	2	3	4	5	6	7	8	9	10	**11**
RI	0	0	0.58	0.9	1.12	1.24	1.32	1.41	1.45	1.49	**1.51**

The CR should be < 0.1; a value above this limit indicates that the consistency matrix is not reliable and needs to be revised (Shahabi et al., 2014).

The performance of the final landslide susceptibility maps will be tested by performing the AUC and the seed cell area index (SCAI index). The SCAI index method was proposed by Suzen and Doyuran (2004) and is equal to the ratio of the percentage area for each landslide susceptibility class to the percentage of an occurred landslide in each class; this method shows the precision of the models in a qualitative way (Abedini et al. 2017). It is viable that the very high and high susceptibility classes to have very small SCAI values, whereas no susceptibility and low susceptibility classes to have higher SCAI values (Sdao et al. 2013; Chen et al. 2016; Abedini et al. 2017).

4.4. Monitoring geomorphological processes – using the newest technologies to assess the degradation of cultural heritage is an important aspect in determining the rate of erosion (Romanescu and Nicu, 2014; Margottini et al., 2015; Agapiou et al., 2016; Tapete and Cigna, 2017) and management of cultural heritage (Deroin et al., 2017). In this study, modern, high precision equipment was used to survey some of the most important Neolithic sites from the northeastern part of Romania. A series of oblique and vertical aerial photographs were taken using a light sports aircraft in May 2015 and 2017; LIDAR (Megarry et al., 2016; Rodriguez-Gonzalvez et al., 2017) was used to prepare the digital model of terrain and to extract the landslides.

To realise precise surveys of the landslides, a Leica ScanStation HDS 5600 3-D laser scanner, a Leica GPS 1200 System, and a Leica TCR1201 total station were used. All the surveys were made in STEREO 70, the official projection of Romania. They are widely used in monitoring soil erosion processes that are affecting cultural heritage sites (Romanescu et al., 2012; Romanescu and Nicu, 2014; Kincey et al., 2017). Geophysical surveys were made with a 5-probe-array fluxgate gradiometer, which is part of the Sensys system; field data were georeferenced and processed with the help of Geoplot software. The surveys were made to determine whether the surface of the site is affected by landslide processes and to establish the extent of the impact. All the data were integrated into a GIS (Mihu-Pintilie et al., 2016), as being a reliable and precise tool to cope with a high amount of geographical and archaeological data (Neubauer, 2004).

5. Integration of spatial and archaeological data

5.1. Map of landslide inventory

A complete and precise map of landslide inventory is essential for producing high-quality maps of landslide susceptibility, as well as to calibrate and validate the final susceptibility models (Schmaltz et al., 2017). Because no landslide inventories are available in Romania, or for the study area, a complete inventory was made using LIDAR data (survey from 2012) and field investigations. Digitising the landslide polygons, revealed that 23% of the study area was affected by landslide processes; from the total number of 764 landslides, 611 landslides (80%) were randomly selected for model training, and the remaining 153 landslides (20%) were used to test the performance of the model.

5.2. Altitude

Represents a widely used conditioning factor in landslide susceptibility analysis (Chen et al., 2016; Patriche et al., 2016; Wu et al. 2016). Within the study area, a DEM with a resolution of 5x5 m/pixel was used; this parameter was grouped into five classes, as follows 50.2 – 100, 101 – 200, 201 – 300, 301 – 400, and > 401 m (Fig. 3a).

5.3. Land use

Land use has a significant role in triggering landslides, depending on the degree of soil coverage with vegetation; it represents a factor very often used in studies dealing with landslide susceptibility (Roșca et al., 2015; Pham et al., 2017). In the study area the main categories of land use (Fig. 3b) were grouped into four classes of susceptibility: class one (forests, built areas, water bodies, wine yards, inland wetlands, artificial surface), class two (scrubs), class three (arable land), and class four (pastures, agricultural areas). Class four represents the highest susceptibility to landslides.

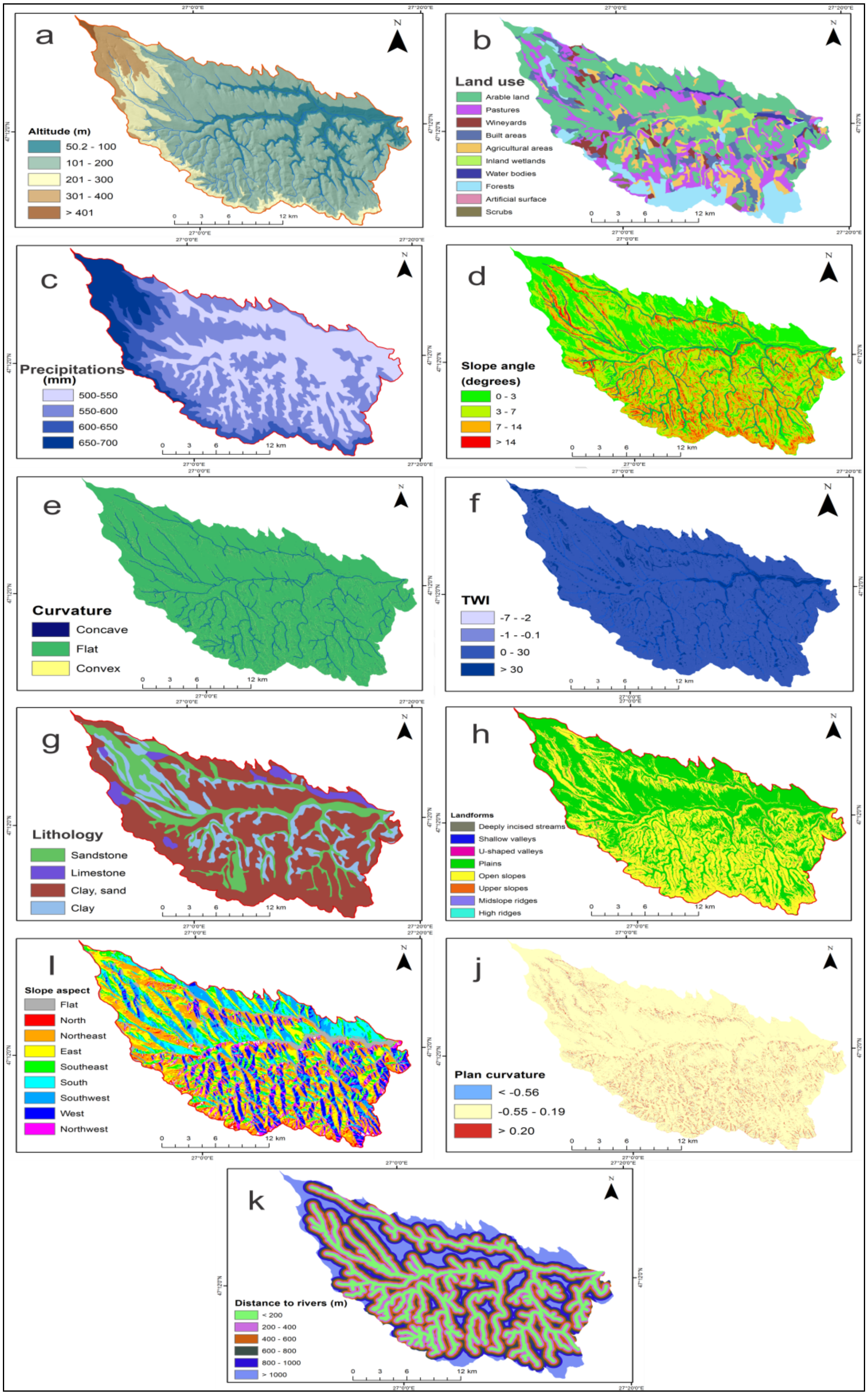
a
Altitude (m)
50.2 - 100
101 - 200
201 - 300
301 - 400
> 401
b
Land use
Arable land
Pastures
Wineyards
Built areas
Agricultural areas
Inland wetlands
Water bodies
Forests
Artificial surface
Scrubs
c
Precipitations (mm)
500-550
550-600
600-650
650-700
d
Slope angle (degrees)
0 - 3
3 - 7
7 - 14
> 14
e
Curvature
Concave
Flat
Convex
f
TWI
-7 - -2
-1 - -0.1
0 - 30
> 30
g
Lithology
Sandstone
Limestone
Clay, sand
Clay
h
Landforms
Deeply incised streams
Shallow valleys
U-shaped valleys
Plains
Open slopes
Upper slopes
Midslope ridges
High ridges
I
Slope aspect
Flat
North
Northeast
East
Southeast
South
Southwest
West
Northwest
j
Plan curvature
< -0.56
-0.55 - 0.19
> 0.20
k
Distance to rivers (m)
< 200
200 - 400
400 - 600
600 - 800
800 - 1000
> 1000
0 3 6 12 km

Figure 3. Landslide conditioning factors and classification. a. Elevation, b. Land use, c. Precipitations, d. Slope angle, e. Curvature, f. Topographic wetness index (TWI), g. Lithology, h. Landforms, i. Slope aspect, j Plan curvature, k. Distance to rivers

5.4. Precipitation

The distribution of precipitation regulates the water content of the soil and is a significant factor in calculating landslide susceptibility (Chen et al., 2016; Zhang et al., 2016). In the study area, the values of this parameter have been concluded according to Minea, 2012, and distributed into four classes (mm/year) (Fig. 3c) 500 – 550, 550 – 600, 600 – 650, and 650 – 700. Precipitation ranging between 500 – 600 mm/year are spread on cca. 80% of the total surface of the basin. Higher precipitation is specific to the plateau area located in the northwestern part of the catchment.

5.5. Slope angle

Slope angle is considered to be one of the most important factors when it comes to slope stability, being frequently used in preparing landslide susceptibility maps (Bălteanu et al., 2010; Youssef et al., 2015; Chen et al., 2016; Zhang et al., 2016; Nicu, 2017a; Pawluszek and Borkowski, 2017). This parameter is derived from the DEM with the help of ArcGIS Spatial Analyst Tools. In the study area the slope was divided into four classes using Natural Breaks (Jenks) classification 0-3, 3-7, 7-14, >14 (Fig. 3d).

5.6. Curvature

The curvature is defined as the rate of change of slope gradient in a particular direction; the values represent the morphology of the topography (Lee et al. 2004, Wang et al., 2016). Negative curvature represents concave, zero curvature represents flat, and positive curvature represents convex areas; therefore, the map was classified into three classes (Fig. 3e).

5.7. Topographic wetness index

The topographic wetness index (TWI) represents the effect of topography on the size and location of saturated source areas of runoff triggering; this parameter was developed in a rainfall-runoff model named TOPMODEL (Beven and Kirkby, 1979). The soil moisture affects the material on the slopes, thus, diminishing soil stability. It is a common factor used in landslide studies (Wang et al., 2016; Zhang et al., 2016), and can be calculated using the following formula

$$TWI = log_e \, (A \, / \, b\tan\beta) \qquad \text{(Eq. 6)}$$

where A is the flow accumulation in square meters, b is the width of the pixel through which the water flows in meters, and β is the slope (Beven and Kirkby, 1979). In the study area, the topographic wetness index was calculated and classified into four classes using Natural Breaks (Jenks) method -7 – -2, -1 – -0.1, 0 – 30, > 30 (Fig. 3f).

5.8. Lithology

The characteristics of lithological units represent the base on which landslides are occurring (Feizizadeh and Blaschke, 2014; Patriche et al., 2016; Wang et al. 2017). This parameter was extracted from the pedological studies 1:10,000 scale. The basin comprises four main lithological classes: sandstone (Holocene and Bessarabian age), limestone (Pleistocene and Bessarabian age), clay and sand (Bessarabian age), and clay (Bessarabian age). (Fig. 3g).

5.9. Landforms

The landforms parameter was derived with the help of ArcGIS – Topography Tools (Jenness, 2006) and have a high importance in the triggering of landslides (Roșca et al., 2015; Chen et al., 2016). The main landforms are: plains (52%), open slopes (45%), U-shaped valleys (1.3%), upper slopes (1.2%), deeply incised streams (0.06%), high ridges (0.04%), and shallow valleys and mid-slope ridges (0.001%) (Fig. 3h). The landforms with the highest probability of contributing to slope failure are the mid-slope ridges, followed by open slopes, deeply incised streams and shallow valleys.

5.10. Slope aspect

Slope aspect represents another important factor in estimating landslide susceptibility (Patriche et al., 2016; Zhang et al., 2016). Aspect impacts the weather (water resulted from snow melting, rainfall, exposure to sunlight), and land use (pastures, forest, scrubs, arable land). Dominant in the area are north-facing slopes and flat areas (Fig. 3i).

5.11. Plan curvature

Plan curvature represents the rate of change of the slope angle, with immediate effects on surface runoff and the development of landslides. This parameter is usually used to produce landslide susceptibility models (Chen et al., 2016; Wu et al., 2016), and was classified into three classes using Natural Breaks (Jenks) method: < - 0.56, - 0.55 – 0.19, > 0.20 (Fig. 3j).

5.12. Distance to rivers

Distance to rivers parameter is a significant conditioning factor because streams are decreasing slope stability by erosion of slopes (Wang et al., 2016; Zhang et al., 2016; Pham et al., 2017); in the current study, six different buffer classes were created as follows < 200, 200 – 400, 400 – 600, 600 – 800, 800 – 1000, > 1000 m (Fig. 3k).

6. Results and discussion

AHP, FR, and SI were used to calculate the LSI. The surface and distribution (%) of each susceptibility class were calculated for each method. The classes of the LSI are: no susceptibility, low susceptibility, medium, high and very high susceptibility; the final raster (with a 5x5 m/pixel resolution) was reclassified by using the Natural Breaks (Jenks) method. The method with the highest predictability rate, which is SI, was used to evaluate the number of Neolithic sites that are in danger.

6.1. LSI using FR

The values of the FR analysis are summarised in Table 1, column 6. This method selected landforms, TWI, and lithology as being the most important when it comes to slope failures. In

Table 1, column 6, landform classes six and seven, which is open slopes and upper slopes, respectively, have higher frequency ratio weight (0.52 and 0.27, respectively). For the TWI, high-frequency values (0.44) are associated with a positive value (> 0) of the index. When it comes to lithology, clays are the most susceptible to landslides (0.49), followed by the mix of clay and sand (0.29). These three factors are followed by altitude, slope angle, land use, aspect, distance to rivers, curvature, precipitation, and plan curvature, respectively. This means that the final landslide susceptibility map will look more like the map of landforms, TWI and lithology.

The final LSI is calculated and expressed as Fig. 4a. The statistical results using FR are shown in Tab. 4. High and very high classes occupy almost half of the surface of the basin (cca. 47%), which is alarming because of the high density of cultural heritage sites of the area.

6.2. LSI using SI

The relation of each landslide conditioning factor and its spatial relationship with landslide triggering is shown in Tab. 1, column 8. A positive value indicates a high correlation between the class factor and landslide phenomena, whereas negative values highlight a very low correlation with landslide phenomena. High values are related with the following conditioning factors: landforms (mid-slope ridges – 0.34, open slopes – 0.28, high ridges, deeply incised streams, and mid slope drainages – 0.25), slope (> 14 degrees – 0.41, 7-14 degrees – 0.36), precipitations (600-650 mm – 0.29), elevation (201-300 m – 0.22). The final landslide susceptibility map is shown in Fig. 4b. The statistical results using FR are shown in Tab. 4. High and very high classes occupy almost half of the surface of the basin (cca. 49%).

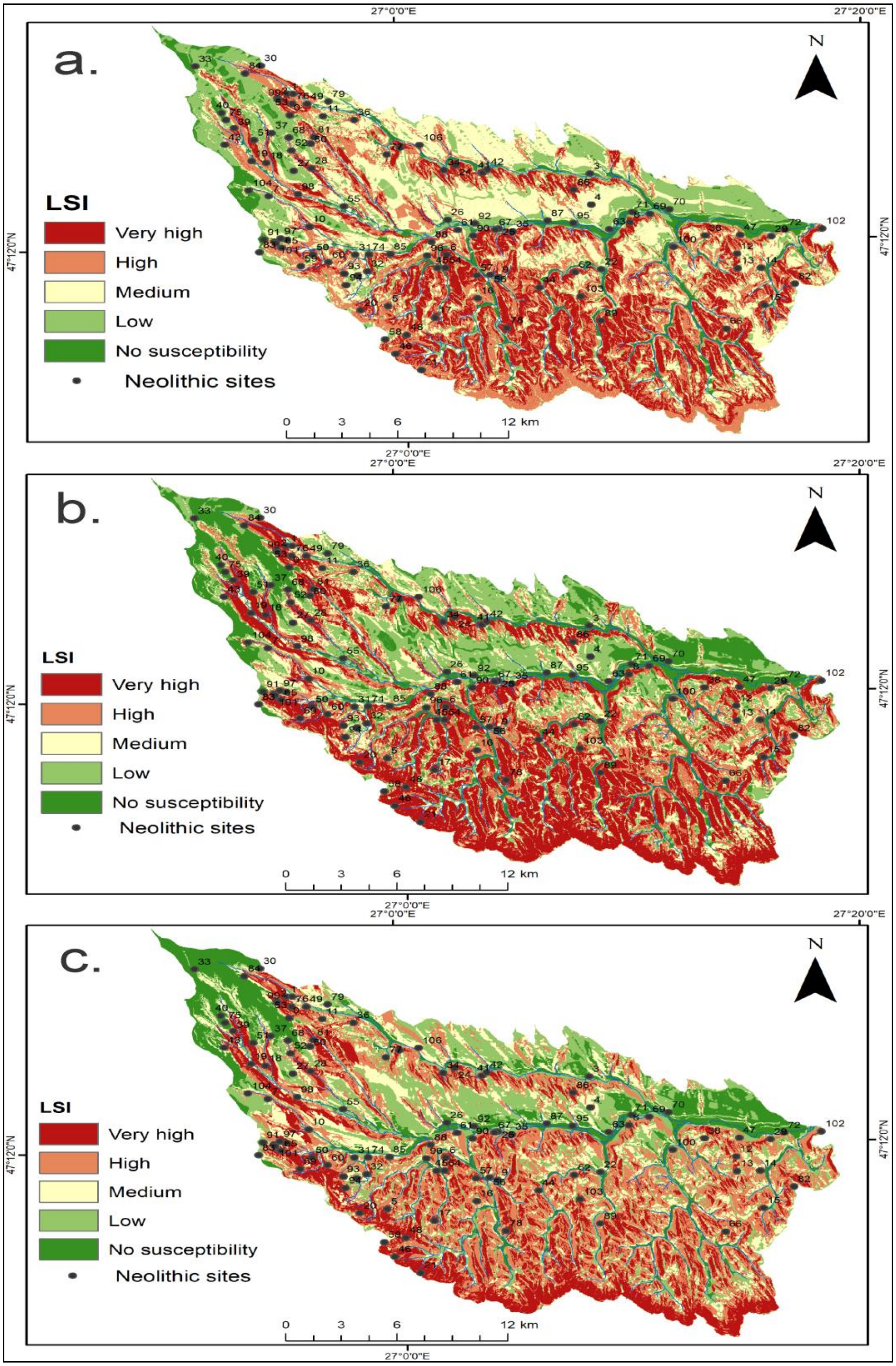

Figure 4. LSI maps produced using: a. FR, b. SI, c. AHP

Table 4. Statistical results of LSI using the three methods

Susceptibility	**Landslide occurrence (FR)**			**Landslide occurrence (SI)**			**Landslide occurrence (AHP)**		
	Count (pixels)	Ratio (%)	Area (km^2)	Count (pixels)	Ratio (%)	Area (km^2)	Count (pixels)	Ratio (%)	Area (km^2)
No susceptibility	1,570,584	7.15	39.26	3,494,339	15.91	87.35	2,766,753	12.59	69.16
Low	3,998,541	18.20	99.96	4,392,062	19.99	109.80	4,757,119	21.66	118.92
Medium	6,094,601	27.75	152.36	3,316,498	15.10	82.91	3,814,702	17.37	95.36
High	5,624,583	25.61	140.61	4,154,073	18.91	103.85	6,542,825	29.79	163.57
Very high	4,672,834	21.27	116.82	6,604,171	30	165.10	4,079,744	18.5	101.99

6.3. LSI using AHP

The comparison matrix, initially based on the expert evaluation, has prioritised the weights of each conditioning factor (Tab. 2). Following the calculation of the weights of each conditioning factor, the CR value was 0.05 (< 0.1); this indicates that the weights obtained are considered reasonable and the final landslide susceptibility maps will have a high accuracy. Among the eleven conditioning factors, the AHP method selected, in decreasing order are: slope (18.9), land use and landforms (13.5), lithology (13.1) and distance to the river (12.1). The final landslide susceptibility map was obtained (Fig. 4c) by summarising the weights of each conditioning factor. The statistical results using FR are shown in Tab. 4.

6.4. Validation and comparison of the LSI maps

A validation of landslide susceptibility maps is needed, in order to check the viability of the final LSI maps (Wang et al., 2017).

6.4.1. AUC method – for the study area, validation and comparison of the landslide susceptibility maps produced with FR, SI and AHP models were checked by using the area under curvature (AUC). This method is widely used in studies dealing with the evaluation of landslide susceptibility and creates success rate and prediction rate curves. The success rate curves for the three methods are shown in Fig. 5; it can be observed that the SI model has a higher area under the curve (AUC) value than FR and AHP.

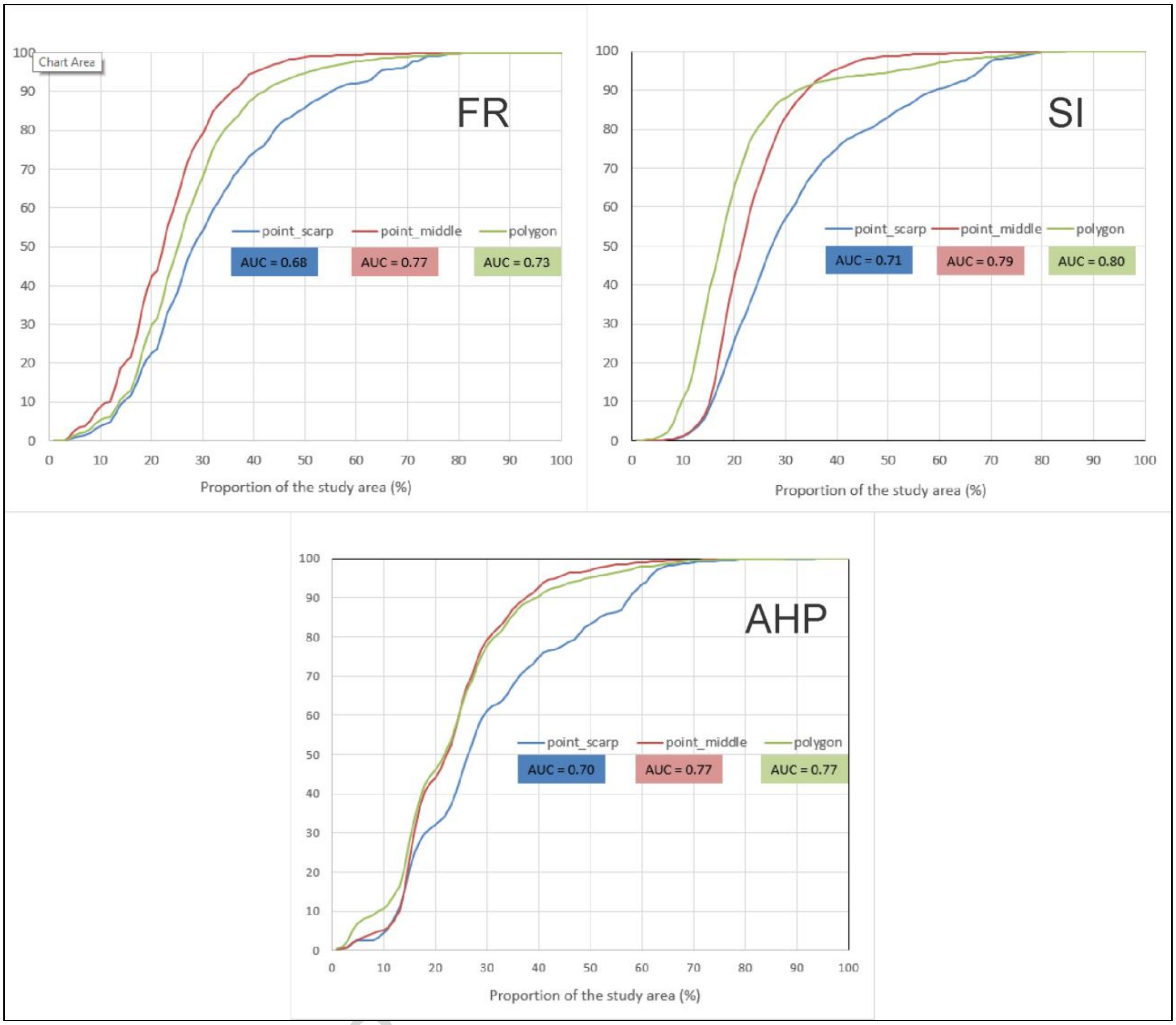

Figure 5. Success rate curves with associated AUC values computed for each diagnostic area of the three models

Regarding the different diagnostic areas used to calculate the success rate, out of the three models, SI model has the highest value (AUC $_{point\_scarp}$ = 71.24%, AUC $_{point\_middle}$ = 79.19%, AUC $_{polygon}$ = 80.17%) than the FR model (AUC $_{point\_scarp}$ = 68.52%, AUC $_{point\_middle}$ = 77.61%, AUC $_{polygon}$ = 73.60%) and AHP model (AUC $_{point\_scarp}$ = 70.17%, AUC $_{point\_middle}$ = 77.24%, AUC $_{polygon}$ = 77.33%).

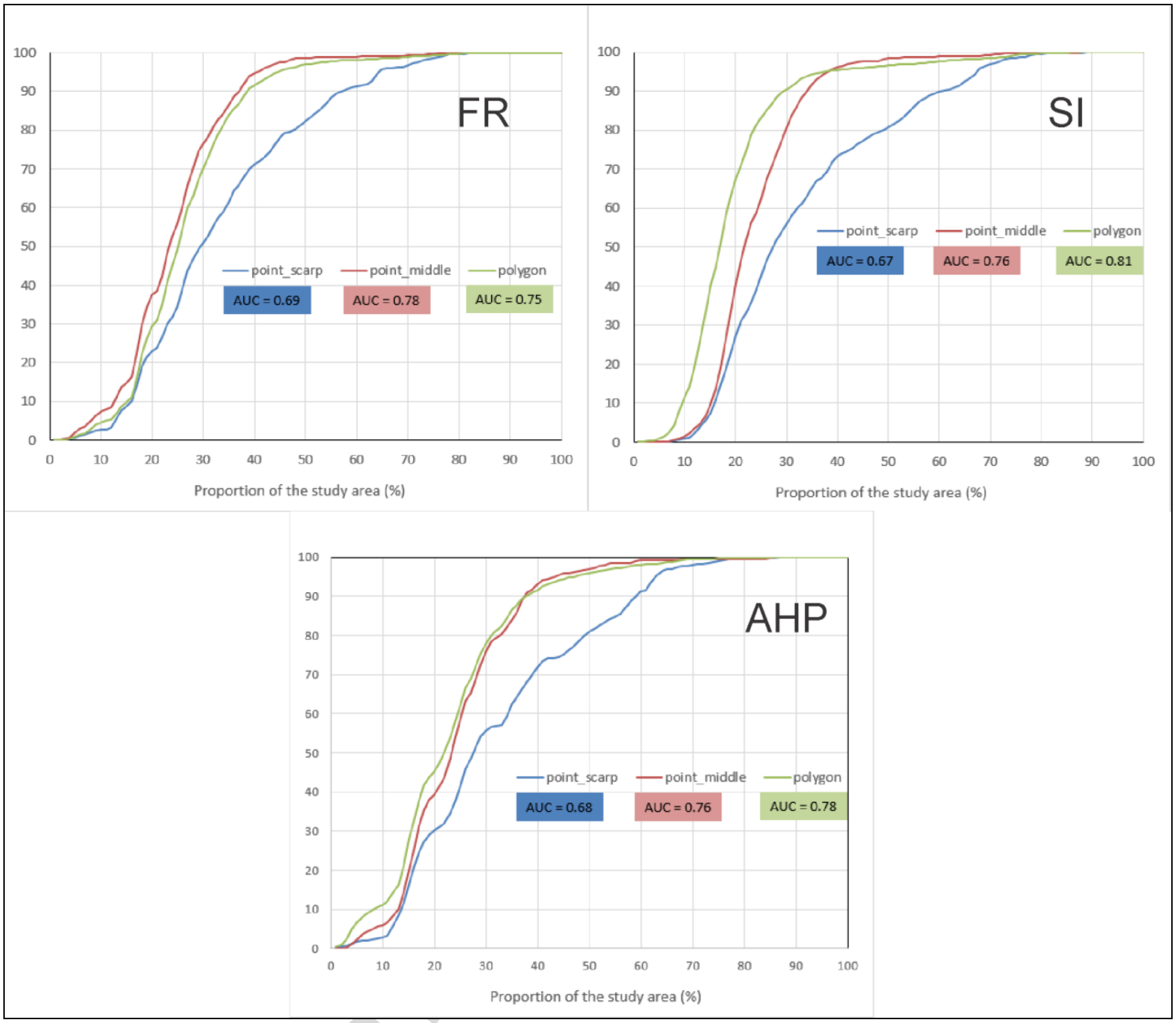

Figure 6. Prediction rate curves with associated AUC values computed for each diagnostic area of the three models

The prediction rate curve shows that the highest prediction accuracy for all the three diagnostic areas belongs to SI method (Fig. 6) (AUC $_{point\_scarp}$ = 67.65%, AUC $_{point\_middle}$ = 76.70%, AUC $_{polygon}$ = 81.18%), when comparing with FR, AUC $_{point\_scarp}$ = 69.52%, AUC $_{point\_middle}$ = 78.32%, AUC $_{polygon}$ = 75.16%) and AHP models, (AUC $_{point\_scarp}$ = 68.33%, AUC $_{point\_middle}$ = 76.35%, AUC $_{polygon}$ = 78.57%). As it can be observed, the landslide area had a better success and prediction rate; other studies reported landslide areas as having a weak performance (Rotigliano et al., 2011). This resulted from the difference in years of the DEM and of the landslide inventory used. Regarding the diagnostic areas for predictive strenghtness, landslide area is followed by the points located in the middle of the landslide. The area is considered more dynamic and the slope is already modified; therefore, better results than the points located on the scarp.

Table 5. The densities of landslide occurrence (SCAI) for AHP, FR and SI models

Validation method	**Class**	**Pixel number**	**Area (%)**	**Number of landslides**	**Landslides (%)**	**SCAI**
AHP	Very high	4,079,744	18.59	244	31.93	0.58
	High	6,542,825	29.79	282	36.94	0.80
	Medium	3,814,702	17.37	123	16.09	1.07
	Low	4,757,119	21.66	107	14	1.54
	No susceptibility	2,766,753	12.59	8	1.04	12.10
FR	Very high	4,672,834	21.27	289	37.82	0.56
	High	5,624,583	25.61	274	35.86	0.71
	Medium	6,094,601	27.75	135	17.67	1.57
	Low	3,998,541	18.20	58	7.59	2.39
	No susceptibility	1,570,582	7.15	8	1.04	6.87

SI	Very high	6,604,171	30.07	354	46.33	0.64
	High	4,154,073	18.91	222	29.05	0.65
	Medium	3,316,498	15.10	111	14.53	1.03
	Low	4,392,062	19.99	62	8.13	2.45
	No susceptibility	3,494,339	15.91	15	1.96	8.11

6.4.2. SCAI (seed cell area index method) – another method to assess the reliability of the landslide susceptibility models realised with AHP, FR, and SI models is represented by the seed cell area index (SCAI) method. Tab. 5 shows that high and very high susceptibility classes have very low SCAI values (<1), whereas low susceptibility and no susceptibility classes have high, respectively, very high values. This means that the results of the maps are accurate.

6.5. Neolithic sites in danger

A buffer zone of 100 m was made for each point to obtain an average surface of 3 ha for each settlement; this is considered the average surface of a Neolithic settlement (Asăndulesei, 2017). Cases occur, however, in which the surface is larger (in the case of the hilltop or fortified settlements) or smaller (settlements that have only one layer of habitation). Therefore, we decided to choose the surface of 3 ha as being pertinent to our study.

Out of the total number of 107 settlements, 41 sites are found in areas with very high susceptibility, 30 sites in areas with high susceptibility, 19 in medium susceptibility areas, 8 in low susceptibility areas, and 9 in no susceptibility areas. As it can be observed, approximately 70% of the Neolithic sites are located in areas with high and very high susceptibility to landslides. This means that the Neolithic sites are in real danger in the future. The location of Neolithic settlements in areas with high susceptibility to landslides is because one of the main landforms preferred by the prehistoric people were hilltops (usually surrounded by steep slopes with a defensive purpose).

6.5.1. Costești settlement (*Cier / La Școală*), a well-known Neolithic (Fig. 2c) site within the archaeological community in Romania, is located on the right side of Bahluieț river, on a relict landslide deposit, and is now being eroded by the river. This is one of the most researched Cucuteni sites in the northeastern part of the country, because it has a long habitation period, starting with Cucuteni A (cca. 4525/4500 – 3950 CAL. BC) (Bem, 2000) until 15^{th}-17^{th} century.

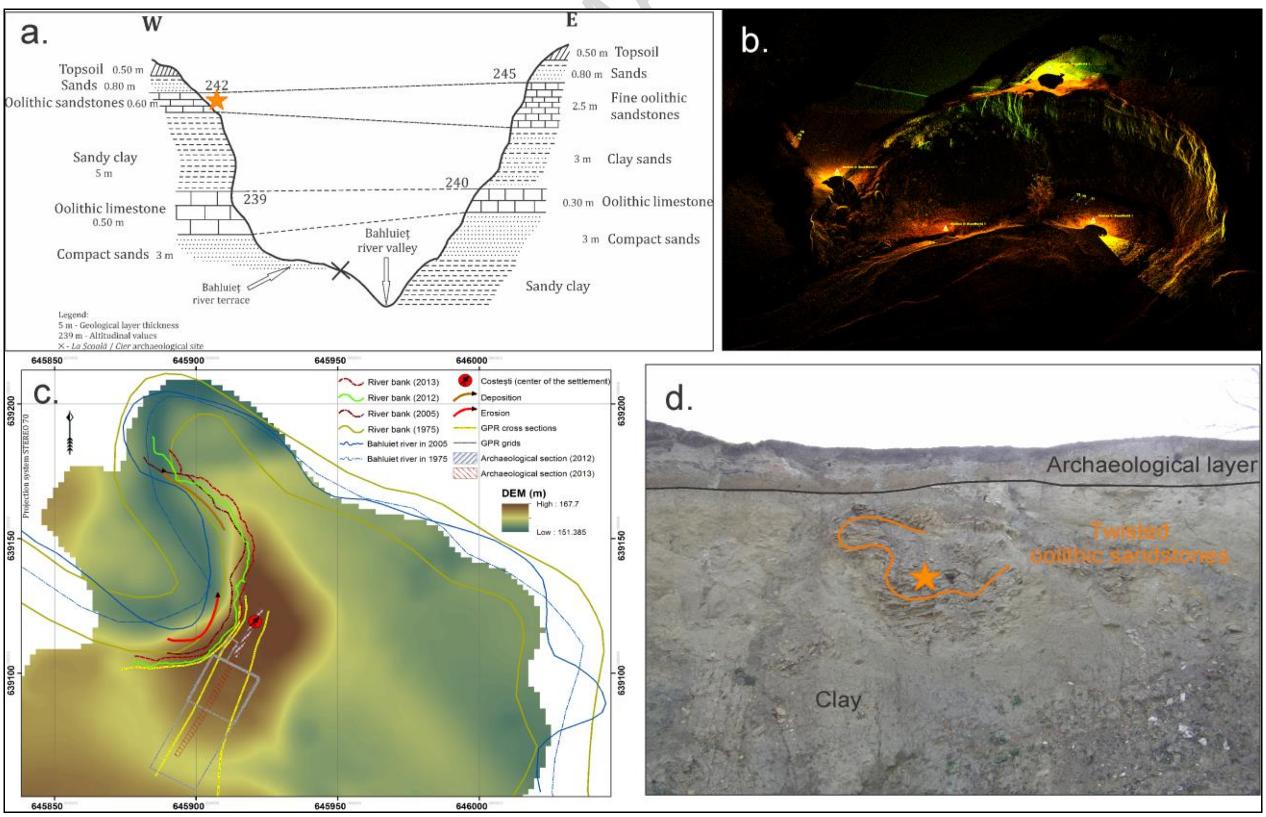

Figure 7. Costești settlement (*Cier / La Școală*) details: 7a. Geological details highlighting the alternation of geological layers, 7b. 3D laser scanner detail, part of the monitoring process, 7c. Detail of the surveys undertaken to establish the erosion of the site, 7d. Detail showing the twisted oolithic limestone, as a proof of the landslide intensity process

Besides the landslide, the western part of the settlement is affected by the erosion of Bahluieț River; the erosion is accentuated by rain with a torrential character, which have a higher density during the last decades. The landslide affecting the site, dated as a very old one (Niculiță et al., 2016) was triggered because of the alternation of geological layers (Fig. 7a) (sands, sandstones, clay, limestone and sands). In time, the site has gradually degraded because of the continuous action of Bahluieț River; a series of historical maps, topographic and 3-D laser scanner surveys (Fig. 7b) were used to monitor the dynamics of Bahluieț riverbed, along with a (Fig. 7c). An analysis resulted in an annual rate of erosion of the western part of the settlement of – 0.26 m/year. After the landslide, the river formed a meander that was used by the prehistoric people as a defensive system; the landslide had packs of rolling sandstone visible in the section dug by Bahluieț River (Fig. 7d). Based on the analysis of the historical maps and modern surveys, the site is about 50% destroyed. It can be observed that the river course has more cut-off meanders in 2005, compared with 1975. Erosion from flowing water spreads from the spill to spring and has the natural tendency to reduce the slope and achieve the equilibrium profile. Moreover, the archaeological excavations that took place in time, contributed to the degradation of the site.

6.5.2. Dealul Boghiu settlement (*Dealul Mare / Filiași*) – represents the typical characteristics of a Neolithic settlement: plateau placement with good visibility, proximity towards Oii river, and the existence of two springs.

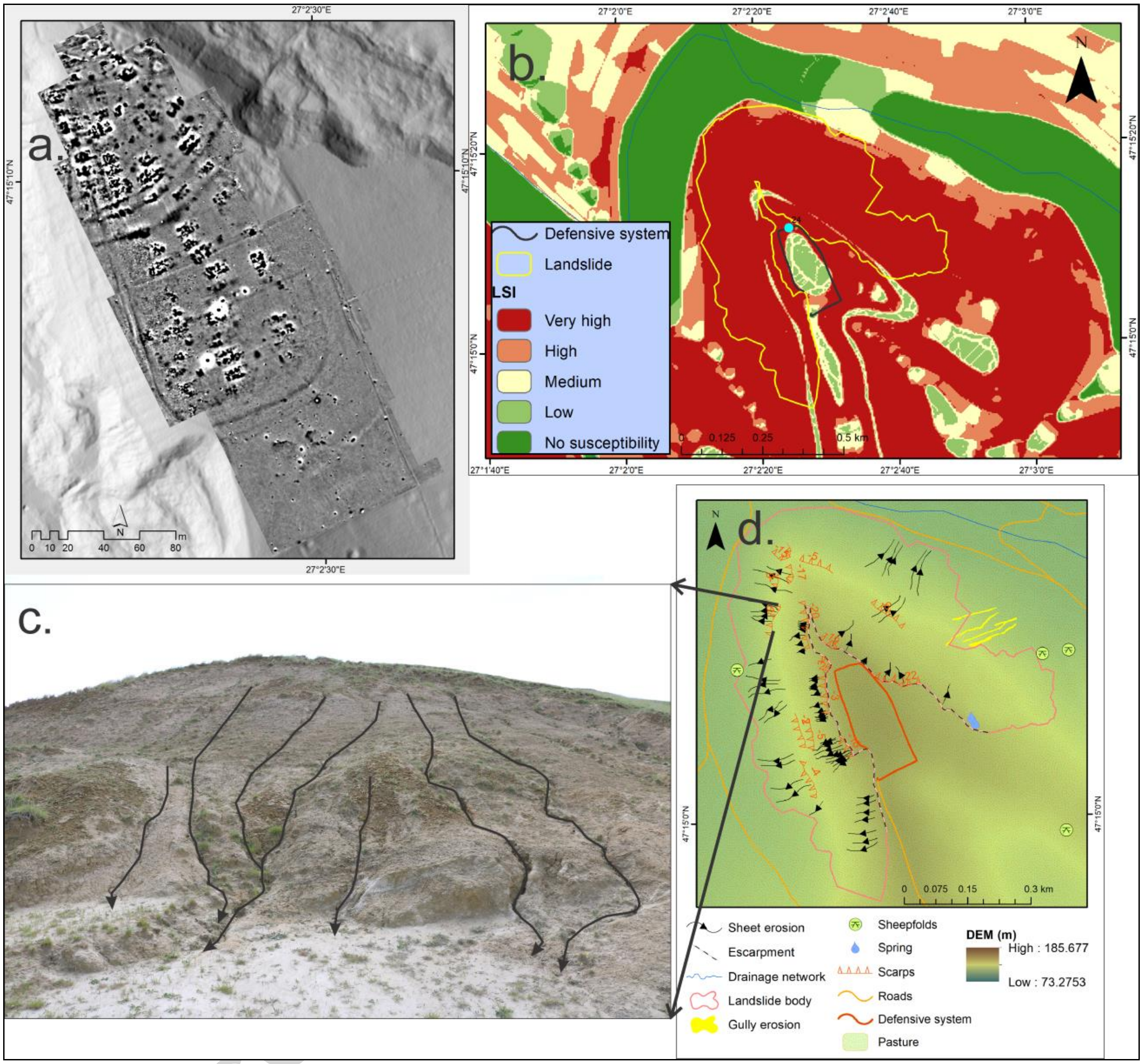

Figure 8. Dealul Boghiu settlement (*Dealul Mare / Filiași*); 8a. Fluxgate gradiometer survey (–10 to + 10, white to black) superimposed on a hillshade derived from LiDAR DEM; 8b. The site overlapping the landslide susceptibility model produced with the SI method; 8c. Sheet erosion from the northwestern part of the settlement; 8d. Geomorphologic and anthropic details

On the plateau the inhabitants were able to practice agriculture. Recent research (Nicu, 2016b; Asăndulesei, 2017) has shown that the settlement had a defensive system which was maintained on a regular basis and the surface outside the fortified area had houses placed in three rows – which is a typical pattern for Cucuteni settlements (Fig. 8a). Settlements with a defensive system were very important in a Neolithic community; therefore, the historical value is high and should be preserved. The plateau area has a low susceptibility to landslides, whereas north, eastern, western, southeastern part of the site has a very high susceptibility to landslides (Fig. 8b). Sheet erosion is affecting the entire surface of the landslide (Fig. 8c), being pronounced by the scarps (having from – 2 to – 22 m in length) located on the entire landslide body. In this way, a considerable amount of flint and ceramic pieces are carried down the slope. Fig. 8d shows all the geomorphological processes and anthropic elements associated around the site.

6.5.3. Dealul Ruginii settlement – represents a new settlement discovered after the analysis of aerial images from May 2017. The site is not officially registered and no archaeological excavations have been completed. This site is affected by landslides and we decided to make geophysical surveys to establish whether the settlement is of Neolithic age or not. Following the geophysical survey (Fig. 9a), it was established that the settlement is of the Neolithic age, with a perimeter of 600 m and a surface of 22415 m^2 (2.2415 ha). We could not establish a precise date for this settlement; further research is needed for this settlement. Our preliminary research referred only to the existence of a settlement in this location, and primary analysis of aerial images and geophysical survey. The north, west and eastern part of the site is located in an area with high susceptibility to landslides, according to our maps (Fig. 9b); the northwestern part, where the slope is very steep, sheet erosion is also affecting the settlement.

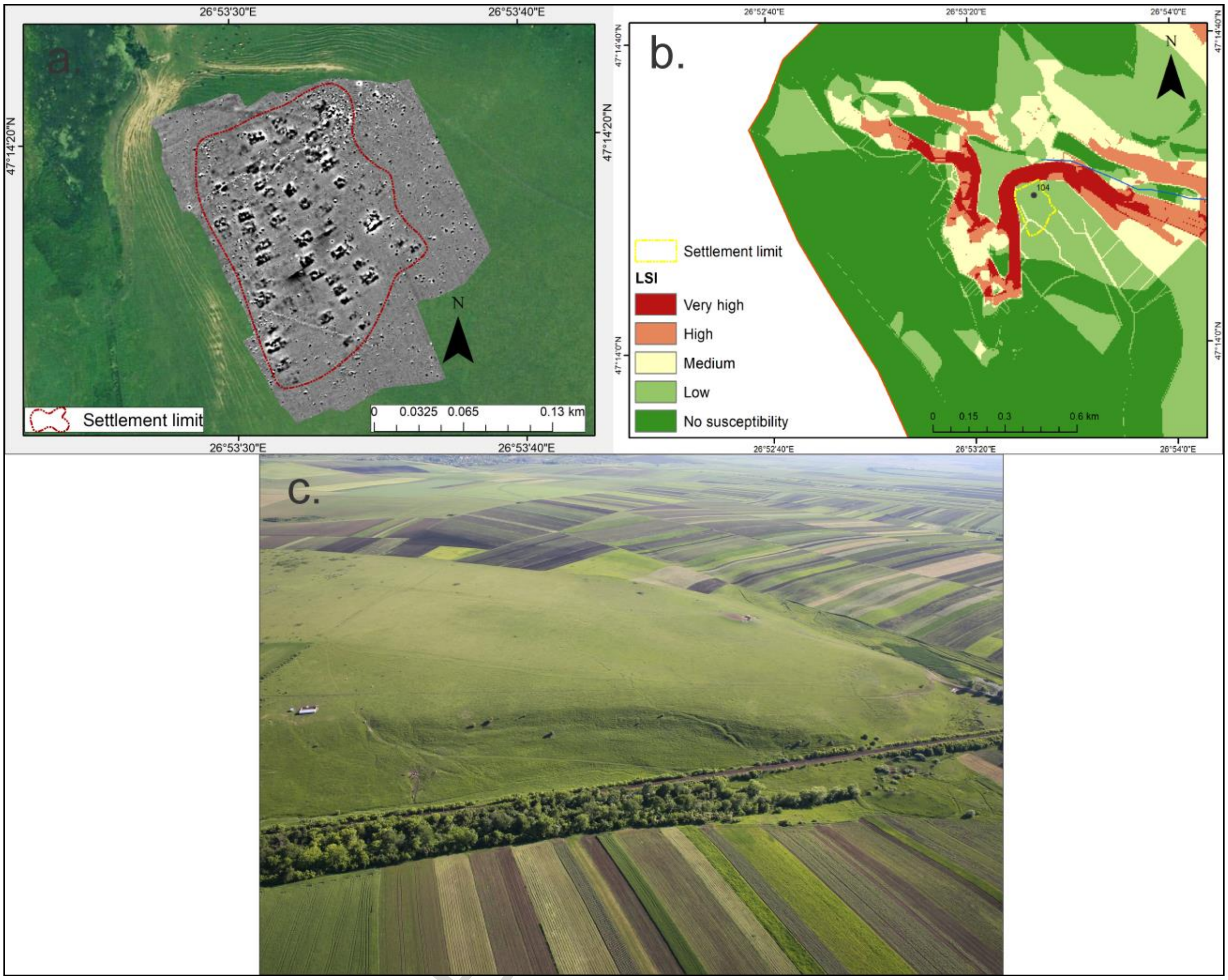

Figure 9. Dealul Ruginii settlement; 9a. Fluxgate gradiometer survey (– 10 to + 10, white to black) superimposed on an orthorectified aerial image; 9b. The site overlapping the landslide susceptibility model; 9c. Aerial photo of the settlement

The general view of the site (Fig. 9c) shows the landscape, which is typical for the northeastern part of Romania (agricultural lands); on the surface of the site are placed a number of two sheepfolds. Overgrazing accentuates the erosion of the site in the north and western part.

7. Conclusions

In this study, three statistical methods were used to test the predictive strenghtness of three different diagnostic areas (scarp, middle of the landslide, landslide area), using 11 conditioning factors. The landslide area had a better success and prediction rate than the scarp and middle of the landslide. The validation results by ROC method shows that the area under the curve for FR, SI, and AHP models (landslide area) are 0.73 (73.60%), 0.80 (80.17%), 0.77 (77.33%) with a prediction accuracy of 0.75 (75.16%), 0.81 (81.18%), and 0.78 (78.57%), respectively. On the other hand, SCAI method has shown a good accuracy of the landslide susceptibility maps produced. Analysing the landslide susceptibility maps, it can be observed that approximately 70% of the sites are located in areas with high and very high susceptibility to landslides. This means that the Neolithic sites in the study area are in real danger. This is a recommendation to the local authorities: analyse the susceptibility maps and propose mitigation measures. Another use of the landslide susceptibility maps is to plan the economic activities, minimise damages costs, environmental and cultural heritage protection, a better management of water resources, hazard mitigation.

Acknowledgements

We are grateful to the Prut-Bârlad Water Administration who provided us with the LIDAR data. James S. Williamson (Memorial University of Newfoundland, Canada) is kindly acknowledged for the English language editing of the manuscript. Many thanks for the constructive comments of two anonymous reviewers.

Declaration of interest: none.

References

Abedini, M., Ghasemyan, B., Rezaei Mogaddam, M.H., 2017. Landslide susceptibility mapping in Bijar city, Kurdistan Province, Iran: a comparative study by logistic regression and AHP models. Environ. Earth. Sci. 76, 308. doi:10.1007/s12665-017-6502-3.

Aburas, M.M., Ho, Y.M., Ramli, M.F., Ash'aari, Z.H., 2017. Improving the capability of an integrated CA-Markov model to simulate spatio-temporal urban growth trends using an Analytic Hierarchy Process and Frequency Ratio. Int. J. Appl. Earth Obs. 59, 65–78.

Agapiou, A., Lysandrou, V., Themistocleous, K., Hadjimitsis, D.G., 2016. Risk assessment of cultural heritage sites clusters using satellite imagery and GIS: the case study of Paphos District, Cyprus. Nat. Hazards 83(1), 5–20.

Ahmad, S., Tahar, R.M., 2014. Selection of renewable energy sources for sustainable development of electricity generation system using analytic hierarchy process: A case of Malaysia. Renew. Energ. 63, 458–466.

Akgün, A., Dag, S., Bulut, F., 2008. Landslide susceptibility mapping for landslide prone area (Findikli, NE of Turkey) by likelihood-frequency ratio and weighted linear combination models. Environ. Geol. 54, 1127–1143. doi:10.1007/s00254-007-0882-8.

Althuwaynee, O.F., Pradhan, B., Park, H.-J., Lee, J.H., 2014. A novel ensemble bivariate statistical evidential belief function with knowledge-based analytical hierarchy process and multivariate statistical logistic regression for landslide susceptibility mapping. Catena 114, 21–36. doi:10.1016/j.catena.2013.10.011.

Al-sharif, A.A.A., Pradhan, B., 2016. Spatio-temporal prediction of urban expansion using bivariate statistical models: assessment of the efficacy of evidential belief functions and frequency ratio models. Appl. Spat. Anal. Polic. 9(2), 213–231.

Armaş, I., Vartolomei, F., Stroia, F., Braşoveanu, L., 2014. Landslide susceptibility deterministic approach using geographic information systems: application to Breaza town, Romania. Nat. Hazards 70, 995–1017. doi:10.1007/s11069-013-0857-x.

Asăndulesei, A., 2017. Inside a Cucuteni settlement: remote sensing techniques for documenting an unexplored Eneolithic site from Northeastern Romania. Remote Sens. 9, 41.

Bălteanu, D., Chendeş, V., Sima, M., Enciu, P., 2010. A country-wide spatial assessment of landslide susceptibility in Romania. Geomorphology 124, 102–112. doi:10.1016/j.geomorph.2010.03.005.

Bem, C., 2000. Elemente de cronologie radiocarbon. Ariile culturale Boian-Gumelniţa-Cernavodă I şi Precucuteni-Cucuteni. Cercetări Arheologice XI, 337–369.

Beven, K.J., Kirkby, M.J., 1979. A physically based, variable contributing area model of basin hydrology. Hydrolog. Sci. J. 24(1), 43–69.

Boghian, D., Enea, S.-C., Pîrnău, R., 2016. The dynamics of Precucuteni and Cucuteni habitat of the Bahluieţ basin (Târgu Frumos Microregion). In: Cucuteni Culture within the European Neo-Eneolithic context (eds. Preoteasa, C., Nicola, C.-D.), Piatra-Neamţ, pp. 411–460.

Cao, C., Xu, P., Wang, Y., Chen, J., Zheng, L., Niu, C., 2016. Flash flood hazard susceptibility mapping using frequency ratio and statistical index methods in coalmine subsidence areas. Sustainability 8, 948.

Chen, W., Li, W., Chai, H., Hou, E., Li, X., Ding, X., 2016. GIS-based landslide susceptibility mapping using analytical hierarchy process (AHP) and certainty factor (CF) models for the

Baozhong region of Baoji City, China. Environ. Earth Sci. 75, 63. doi:10.1007/s12665-015-4795-7.

Choi, J., Oh, H.-J., Lee H.-J., Lee, C., Lee, S., 2012. Combining landslide susceptibility maps obtained from frequency ratio, logistic regression, and artificial neural network models using ASTER images and GIS. Eng. Geol. 124, 12–23.

Clerici, A., Perego, S., Tellini, C., Vescovi, P., 2002. A procedure for landslide susceptibility zonation by the conditional analysis method. Geomorphology 48, 349–364.

Dailey, L.A., Fuhrmann, S., 2017. GIS-based logistic regression for landslide susceptibility analysis in Western Washington State. International Journal of Applied Geospatial Research 8(2), 1–19.

Deroin, J.-P., Kheir, R.B., Abdallah, C., 2017. Geoarchaeological remote sensing survey for cultural heritage management. Case study from Byblos (Jbail, Lebanon). J. Cult. Herit. 23, 37–43.

Feizizadeh, B., Blaschke, T., 2014. An uncertainty and sensitivity analysis approach for GIS-based multicriteria landslide susceptibility mapping. Int. J. Geograf. Inf. Sci. 28(3), 610–638.

Guzzetti, F., Carrara, A., Cardinali, M., Reichenbach, P., 1999. Landslide hazard evaluation: a review of current techniques and their application in a multi-scale study, Central Italy. Geomorphology 31, 181–216.

Guzzetti, F., Reichenbach, P., Cardinali, M., Galli, M., Ardizzone, F., 2005. Probabilistic landslide hazard assessment at the basin scale. Geomorphology 72, 272–299.

Guzzetti, F., Reichenbach, P., Ardizzone, F., Cardinali, M., Galli, M., 2016. Estimating the quality of landslide susceptibility models. Geomorphology 81(1-2), 166–184.

Hong, H., Naghibi, S.A., Dashtpagerdi, M.M., Pourghasemi, H.R., Chen, W., 2017. A comparative assessment between linear and quadratic discriminant analyses (LDA-QDA) with frequency ratio and weights-of-evidence models for forest fire susceptibility mapping in China. Arab. J. Geosci. 10, 167.

Jenness, J., 2006. Topographic Position Index (tpi_jen.avx) extension for ArcView 3.x, v. 1.2. Jenness Enterprises.

Kincey, M., Gerrard, C., Warburton, J., 2017. Quantifying erosion of 'at risk' archaeological sites using repeat terrestrial laser scanning. J. Archaeol. Sci. Rep. 12, 405–424.

Klimeš, J., 2013. Landslide temporal analysis and susceptibility assessment as bases for landslide mitigation, Machu Picchu, Peru. Environ. Earth Sci. 70, 913–925.

Kumar, S., Snehmani, Srivastava, P.K., Gore, A., Singh, M.K., 2016. Fuzzy-frequency ratio model for avalanche susceptibility mapping. Int. J. Digit. Earth. DOI:10.1080/17538947.2016.1197328.

Lazarovici, C.M., Lazarovici, G., 2009. Cucuteni. A Great Civilization of the Prehistoric World. Editura Palatul Culturii, Iași, România.

Lee, S., Choi, J., Min, K., 2004. Probabilistic landslide hazard mapping using GIS and remote sensing data at Boun, Korea. Int. J. Remote Sens. 25, 2037–2052.

Lee, S., Pradhan, B., 2007. Landslide hazard mapping at Selangor, Malaysia using frequency ratio and logistic regression models. Landslides 4, 33–41.

Lin, G.-F., Chang, M.-J., Huang, Y.-C., Ho, J.-Y., 2017. Assessment of susceptibility to rainfall-induced landslides using improved self-organizing linear output map, support vector machine, and logistic regression. Eng. Geol. 224, 62–74.

Lombardo, L., Cama, M., Conoscenti, C., Märker, M., Rotigliano, E., 2015. Binary logistic regression versus stochastic gradient boosted decision trees in assessing landslide susceptibility for multiple-occurring landslide events: application to the 2009 storm event in Messina (Sicily, southern Italy). Nat. Hazards 79(3), 1621–1648. doi:10.1007/s11069-015-1915-3.

Macarovici, N., Turculeț, N., 1956. Geologia regiunii Ruginoasa – Hărmănești – Vașcani – Costești (Raionul Tg. Frumos) (extras). An. Șt. Ale Univ. “Al. I. Cuza” din Iași 2(2), 287–295.

Margottini, C., Fidolini, F., Iadanza, C., Trigila, A., Ubelmann, Y., 2015. The conservation of the Shahr-e-Zohak archaeological site (central Afghanistan): Geomorphological processes and ecosystem-based mitigation. Geomorphology 239, 73–90.

Mărgărint, M.C., Grozavu, A., Patriche, C.V., 2013. Assessing the spatial variability of coefficients of landslide predictors in different regions of Romania using logistic regression. Nat. Hazards Earth Syst. Sci.13, 3339–3355. doi:10.5194/nhess-13-3339-2013.

Megarry, W.P., Davenport, B.A., Comer, D.C., 2016. Emerging applications of LiDAR / Airborne Laser Scanning in the management of World Heritage Sites. Conserv. Manage. Archa. 18(4), 393–410.

Meng, Q., Miao, F., Zhen, J., Wang, X., W, A., Peng, Y., Fan Q., 2016. GIS-based landslide susceptibility mapping with logistic regression, analytical hierarchy process, and combined fuzzy and support vector machine methods: a case study from Wolong Giant Panda Natural Reserve, China. B. Eng. Geol. Environ. 75(3), 923–944.

Mihai, B., Săvulescu, I., Șandric, I., Chițu, Z., 2014. Integration of landslide susceptibility assessment in urban development: a case study in Predeal town, Romanian Carpathians. Area 46(4), 377–388. doi:10.1111/area.12123.

Mihu-Pintilie, A., Asăndulesei, A., Stoleriu, C.C., Romanescu, G., 2016. GIS methods for assessment of hydrogeomorphic risk and anthropogenic impact which affect the archaeological sites. Case study: Dealul Mare archaeological site, Moldavian Plateau (Romania). Acta Geobalcanica 2(1), 35–43.

Minea, I. 2012. Bazinul hidrografic Bahlui. Studiu hidrologic. Editura Universității Alexandru Ioan Cuza Iași, România.

Monah, D., Cucoș, Ș., 1985. Așezările Culturii Cucuteni din România. Editura Junimea, Iași, România.

Monteiro, V., Painho, M., Vaz., E. 2015. Is the heritage really important? A theoretical framework for heritage reputation using citizen sensing. Habitat Int. 45, 156–162.

Mousavi, S.M., Golkarian, A., Naghibi, S.A., Kalantar, B., Pradhan, B., 2017. GIS-based groundwater spring potential mapping using data mining boosted regression tree and probabilistic frequency ratio models in Iran. AIMS Geosciences 3(1), 91–115.

Myronidis, D., Papageorgiou, C., Theoplanous, S., 2016. Landslide susceptibility mapping based on landslide history and analytic hierarchy process (AHP). Nat. Hazards 81, 245–263.

Neubauer, W., 2004. GIS in archaeology – The interface between prospection and excavation. Archaeol. Prospect. 11, 159–166.

Nicu, I.C., Romanescu, G., 2016. Effect of natural risk factors upon the evolution of Chacolithic human settlements in Northeastern Romania (Valea Oii watershed). From ancient time dynamics to present day degradation. Z. Geomorphol. 60(1), 1–9.

Nicu, I.C., 2016a. Cultural heritage assessment and vulnerability using Analytic Hierarchy Process and Geographic Information Systems (Valea Oii catchment, North-eastern Romania). An approach to historical maps. Int. J. Disaster Risk Reduct. 20, 103–111. doi:10.1016/j.ijdrr.2016.10.015.

Nicu, I.C., 2016b. Hydrogeomorphic Risk Analysis Affecting Chalcolithic Archaeological Sites from Valea Oii (Bahlui) Watershed, Northeastern Romania. An Interdisciplinary Approach. Springer International Publishing, Switzerland. doi:10.1007/978-3-319-25709-9.

Nicu, I.C., 2017a. Frequency ratio and GIS-based evaluation of landslide susceptibility applied to cultural heritage assessment. J. Cult. Herit. 28, 172–176. doi:10.1016/j.culher.2017.06.002.

Nicu, I.C., 2017b. Natural hazards – a threat for immovable cultural heritage. A review. International Journal of Conservation Science 8(3), 375–388.

Nicu, I.C., 2017c. Tracking natural and anthropic risks from historical maps as a tool for cultural heritage assessment: a case study. Environ. Earth Sci. 76, 330. doi:10.1007/s12665-017-6656-z.

Nicu, I.C., 2018a. Application of analytic hierarchy process, frequency ratio, and statistical index to landslide susceptibility: an approach to endangered cultural heritage. Environ. Earth. Sci. 77, 79.

Nicu, I.C., 2018b. Natural risk assessment and mitigation of cultural heritage sites in North-eastern Romania (Valea Oii river basin). Area. doi:10.1111/area.12433.

Niculiță, M., Mărgărint, M.C., Santangelo, M., 2016. Archaeological evidence for Holocene landslide activity in the Eastern Carpathian lowland. Quatern. Int. 415, 175–189. doi:10.1016/j.quaint.2015.12.048.

Niculiță, M., Mărgărint, M.C., 2017. Landslides and fortified settlements as valuable cultural geomorphosites and geoheritage sites in the Moldavian Plateau, North-eastern Romania. Geoheritage. doi:10.1007/s12371-017-0261-0.

Patriche, C.V., Pirnau, R., Grozavu, A., Rosca, B., 2016. A comparative analysis of Binary Logistic Regression and Analytical Hierarchy Process for landslide susceptibility assessment in the Dobrovat river basin, Romania. Pedosphere 26(3), 335–350. doi:10.1016/S1002-0160(15)60047-9.

Pawluszek, K., Borkowski, A., 2017. Impact of DEM-derived factors and analytical hierarchy process on landslide susceptibility mapping in the region of Rożnów Lake, Poland. Nat. Hazards 86, 919–952.

Pham, B.T., Bui, D.T., Prakash, I., Nguyen, L.H., Dholakia, M.B., 2017. A comparative study of sequential minimal optimization-based support vector machines, vote feature intervals, and logistic regression in landslide susceptibility assessment using GIS. Environ. Earth Sci. 76, 371.

Poli, S., Sterlacchini, S., 2007. Landslide representation strategies in susceptibility studies using weights-of-evidence modelling technique. Nat. Resour. Res. 16, 121–134. doi:10.1007/s11053-007-9043-8.

Pourghasemi, H.R., Moradi, H.R., Fatemi Aghda, S.F., 2013. Landslide susceptibility mapping by binary logistic regression, analytical hierarchy process, and statistical index models and assessment of their performances. Nat. Hazards 69(1), 749–779. doi:10.1007/s11069-013-0728-5.

Pradhan, B., Lee, S., 2010. Delineation of landslide hazard areas on Penang Island, Malaysia, by using frequency ratio, logistic regression, and artificial neural network models. Environ. Earth Sci. 60, 1037. doi:10.1007/s12665-009-0245-8.

Razavizadeh, S., Solaimani, K., Massironi, M., Kavian, A., 2017. Mapping landslide susceptibility with frequency ratio, statistical index, and weights of evidence models: a case study in northern Iran. Environ. Earth Sci. 76, 499. doi:10.1007/s12665-017-6839-7.

Rodriguez-Gonzalvez, P., Fernandez-Palacios, B.J., Munoz-Nieto, A.L., Arias-Sanchez, P., Gonzalez-Aguilera, D., 2017. Mobile LiDAR System: new possibilities for the documentation and dissemination of large cultural heritage sites. Remote Sens. 9(3), 189.

Romanescu, G., Cotiugă, V., Asăndulesei, A., Stoleriu, C.C., 2012. Use of the 3-D scanner in mapping and monitoring the dynamic degradation of soils: case study of the Cucuteni-Baiceni Gully on the Moldavian Plateau (Romania). Hydrol. Earth Syst. Sci. 16, 953–966. doi:10.5194/hess-16-953-2012.

Romanescu, G., Nicu, I.C., 2014. Risk maps for gully erosion processes affecting archaeological sites in Moldavia, Romania. Z. Geomorphol. 58(4), 509–523. doi:10.1127/0372-8854/2014/0133.

Roșca, S., Bilașco, Ș., Petrea, D., Fodorean, I., Vescan, I., Filip, S., 2015. Application of landslide hazard scenarios at annual scale in the Niraj River basin (Transylvania depression, Romania). Nat. Hazards 77, 1573–1592.

Roșca, S., Bilașco, Ș., Petrea, D., Vescan, I., Fodorean, I., 2016. Comparative assessment of landslide susceptibility. Case study: the Niraj river basin (Transylvania depression, Romania). Geomat. Nat. Haz. Risk 7(3), 1043–1064. doi:10.1080/19475705.2015.1030784.

Rotigliano, E., Agnesi, V., Cappadonia, C., Conoscenti, C., 2011. The role of the diagnostic areas in the assessment of landslide susceptibility models: a test in the Sicilian chain. Nat. Hazards 58, 981–999. doi:10.1007/s11069-010-9708-1.

Saaty, T.L., 1977. A scaling method for priorities in hierarchical structures. J. Math. Psychol. 15, 234–281.

Saaty, T.L., 2000. The fundamentals of decision making and priority theory with the analytic hierarchy process. RWS Publications, Pitsburg.

Samia, J., Temme, A., Bregt, A., Wallinga, J., Guzzetti, F., Ardizzone, F., Rossi, M., 2017. Do landslides follow landslides? Insights in path dependency from a multi-temporal landslide inventory. Landslides 14, 547–558. doi:

Schmaltz, E.M., Steger, S., Glade, T., 2017. The influence of forest cover on landslide occurrence explored with spatio-temporal information. Geomorphology 290, 250–264. doi:

Sdao, F., Lioi, D.S., Pascale, S., Caniani, D., Mancini, I.M., 2013. Landslide susceptibility assessment by using a neuro-fuzzy model: a case study in the Rupestrian heritage rich area of Matera. Nat. Hazards Earth Syst. Sci. 13, 395–407. doi:

Shahabi, H., Khezri, S., Ahmad, B.B., Hasim, M., 2014. Landslide susceptibility mapping at central Zab basin, Iran: A comparison between analytical hierarchy process, frequency ratio and logistic regression models. Catena 115, 55–70. doi:10.1016/j.catena.2013.11.014.

Shirzadi, A., Chapi, K., Shahabi, H., Solaimani, K., Kavian, A., Ahmad, B.B., 2017. Rock fall susceptibility assessment along a mountainous road: an evaluation of bivariate statistic, analytic hierarchy process and frequency ratio. Environ. Earth Sci. 76, 152. doi:

Suzen, L.M., Doyuran, V., 2004. A comparison of the GIS based landslide susceptibility assessment methods: multivariate versus bivariate. Environ. Geol. 45, 665–679. doi:

Taboada-Gonzáles, P., Aguillar-Virgen, Q., Ojeda-Benítez, S., Cruz-Sotelo, S., 2014. Application of analytic hierarchy process in a waste treatment technology assessment in Mexico. Environ. Monit. Assess. 186, 5777–5795. doi:

Tapete, D., Cigna, F., 2017. InSAR data for geohazard assessment in UNESCO World Heritage sites: state-of-the-art and perspectives in the Copernicus era. Int. J. Appl. Obs. Geoinformation 63, 24–32. doi:10.1016/j.jag.2017.07.007.

Vakhshoori, V., Zare, M., 2016. Landslide susceptibility mapping by comparing weight of evidence, fuzzy logic, and frequency ratio methods. Geomat. Nat. Haz. Risk 7(5), 1731–1752. doi:10.1080/19475705.2016.1144655.

Van Westen, C.J, 1997. Statistical landslide hazard analysis. ILWIS 2.1 for Windows application guide. ITC Publication, Endschede, 73–84.

Van Westen, C.J., Castellanos, E., Kuriakose, S.L., 2008. Spatial data for landslide susceptibility, hazard, and vulnerability assessment: an overview. Eng. Geol. 102(3-4), 112–131. doi:10.1016/j.enggeo.2008.03.010.

Xu, C., Dai, F.C., Xu, X.W., Lee, Y.H., 2012. GIS-based support vector machine modelling of earthquake-triggered landslide susceptibility in the Jianjiang River watershed, China. Geomorphology 145-146, 70–80. doi:10.1016/j.geomorph.2011.12.040.

Wang, Q., Li, W., Wu, Y., Pei, Y., Xing, M., Yang, D., 2016. A comparative study on the landslide susceptibility mapping using evidential belief function and weights of evidence models. J. Earth Syst. Sci. 125(3), 645–662.

Wang, F., Xu, P., Wang, C., Wang, N., Jiang, N., 2017. Application of a GIS-based slope unit method for landslide susceptibility mapping along the Longzi River, Southeastern Tibetan Plateau, China. International Journal of Geo-Information 6, 172. doi:10.3390/ijgi6060172.

Wu, Y., Li, W., Liu, P., Bai, H., Wang, Q., He, J., Liu, Y., Sun, S., 2016. Application of analytic hierarchy process for landslide susceptibility mapping in the Gangu County, Gansu Province, China. Environ. Earth Sci. 75, 422. doi:10.1007/s12665-015-5194-9.

Youssef, A.M., Al-Kathery, M., Pradhan, B., 2015. Landslide susceptibility mapping at Al-Hasher Area, Jizan (Saudi Arabia) using GIS-based frequency ratio and index of entropy models. Geosci. J. 19(1), 113–134. doi:10.1007/s12303-014-0032-8.

Zhang, G., Cai, Y., Zheng, Z., Zhen, J., Liu, Y., Huang, K., 2016. Integration of the Statistical Index Method and the Analytic Hierarchy Process technique for the assessment of landslide susceptibility in Huizhou, China. Catena 142, 233–244. doi:10.1016/j.catena.2016.03.028.

Zhang, Z., Yang, F., Chen, H., Wu, Y., Li, T., Li, W., Wang, Q., Liu, P., 2016. GIS-based landslide susceptibility analysis using frequency ratio and evidential belief function models. Environ. Earth Sci. 75, 948. doi:10.1007/s12665-016-5732-0.

Zhou, S., Chen, G., Fang, L., Nie, Y., 2016. GIS-based integration of subjective and objective weighting methods for regional landslides susceptibility mapping. Sustainability 8, 334. doi:10.3390/su8040334.

Highlights:

- Assessment of landslide susceptibility on Neolithic sites in a catchment from Moldavian Plateau, north-eastern Romania
- Comparing the predictive strenghtness of different diagnostic areas using three statistical methods
- The most important factors for landslide triggering in Bahluieț River basin are slope, land use, landforms and lithology
- Approximately 70% of the sites are located in areas with high and very high landslide susceptibility
- The landslide susceptibility maps can be used in hazard mitigation, disaster preparedness, cultural heritage preservation and protection